WILEY-VCH

Evgeny Katz

Signal-Switchable Electrochemical Systems

Materials, Methods, and Applications

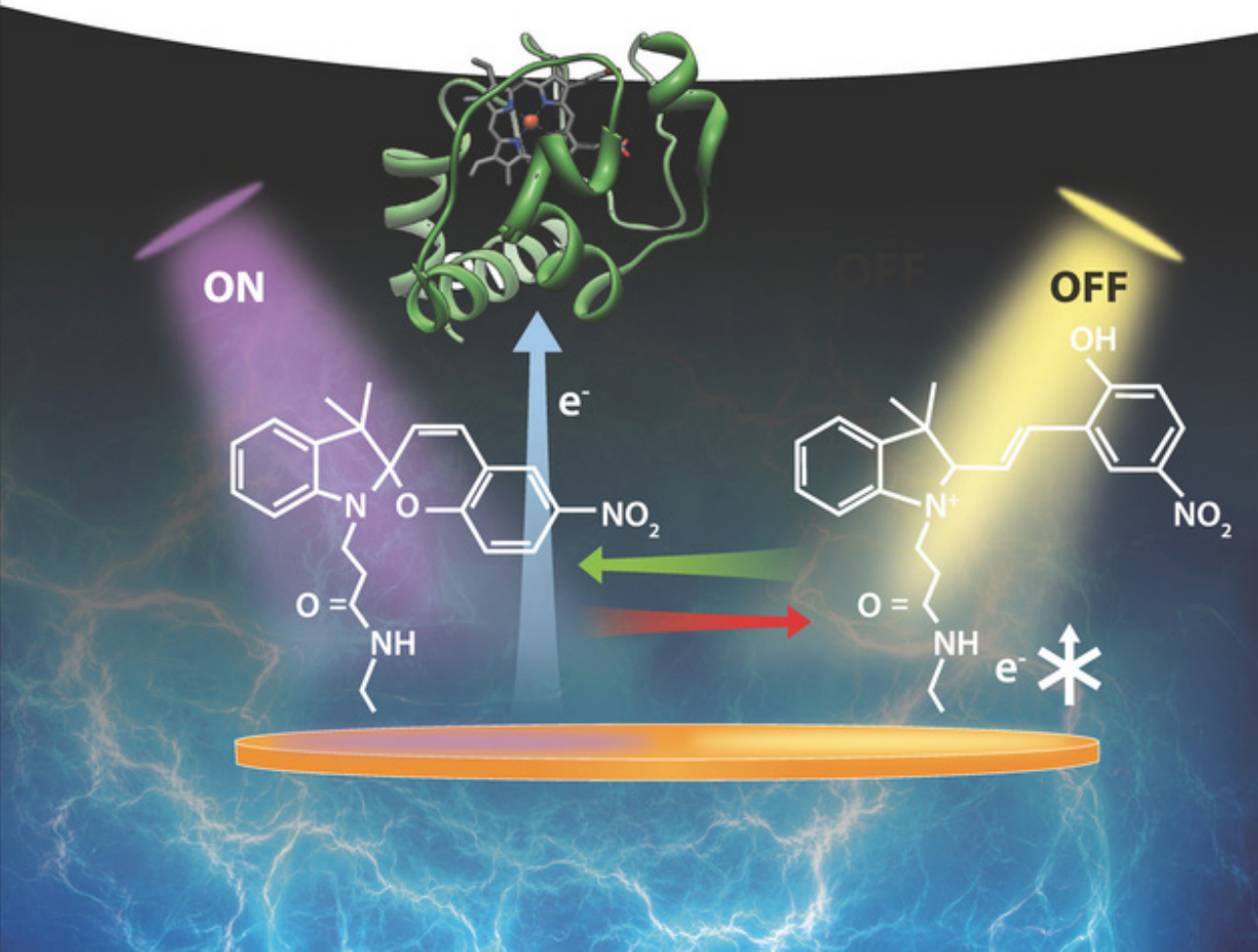

Signal-Switchable Electrochemical Systems

Signal-Switchable Electrochemical Systems

Materials, Methods, and Applications

Evgeny Katz

WILEY-VCH

Author

Dr. Evgeny Katz
Clarkson University
Department of Chemistry and
Biomolecular Science
Clarkson Avenue 8
NY
United States

Cover Images:
Illustration of Cytochrome c by Vossman is licensed under CC BY-SA;
Lightening background © sakkmesterke/iStockphoto

Library of Congress Card No.: applied for

British Library Cataloguing-in-Publication Data
A catalogue record for this book is available from the British Library.

Bibliographic information published by the Deutsche Nationalbibliothek
The Deutsche Nationalbibliothek lists this publication in the Deutsche Nationalbibliografie; detailed bibliographic data are available on the Internet at <http://dnb.d-nb.de>.

Print ISBN: 978-3-527-34545-8
ePDF ISBN: 978-3-527-81875-4
ePub ISBN: 978-3-527-81877-8
Mobi ISBN: 978-3-527-81874-7
oBook ISBN: 978-3-527-81876-1

Typesetting SPi Global, Chennai, India
Printing and Binding

Printed on acid-free paper

10 9 8 7 6 5 4 3 2 1

In the memory of Prof. Ilya Yakovlevich Shaferstain, my first chemistry teacher.

Contents

Preface

Scientific research and engineering in the area of switchable electrodes and complex electrochemical systems, aiming at developing adaptable devices controlled by external signals, have been rapidly progressing in the past two decades, greatly contributing to biomedical and technological advances, thus producing numerous applications. Additionally, this research is absorbing novel achievements and discoveries in materials science, nanotechnology, unconventional computing, and many other science and technology areas. This book overviews the multidisciplinary field of adaptable signal-controlled electrochemical systems and processes highlighting their key aspects and future perspectives. The different topics addressed in this book will be of high interest to the interdisciplinary community active in the areas of electroanalytical and bioelectroanalytical chemistry, biosensors, biofuel cells, signal-processing systems, electrical engineering, etc. It is hoped that the collection of different chapters compiled in this book will be important and beneficial for researchers and students working in various areas of science and engineering. Furthermore, the book is aimed at attracting young scientists and introducing them to the field, while providing newcomers with an enormous collection of literature references and carefully prepared illustrations. I, indeed, hope that the book will spark the imagination of scientists to further develop the topic.

The book summarizes research efforts of many groups from different universities and countries. A significant amount of the discussed material (but obviously not all of it) has originated from the studies to which I have personally contributed. I am very grateful to all scientists, researchers, and students who have participated in this research and have made the achieved results possible. Also, I would like to thank the whole editorial team of Wiley-VCH for its highly professional, effective and pleasant in communication work on the book, making very fast book preparation and publication possible.

It should be noted that the field of signal-controlled electrochemical systems relates in some extent to the fascinating areas of unconventional computing and implantable bioelectronics, which consideration is outside the scope of this book. These complementary areas of molecular/biomolecular computing and electronic engineering were covered in three other recent books published by Wiley-VCH: [1–3].

I would like to conclude this preface by thanking my wife Nina for her support in every respect in the past 46 years. Without her help it would not have been possible to complete this work.

References

1 Katz, E. ed. (2012). *Molecular and Supramolecular Information Processing: From Molecular Switches to Logic Systems*. Weinheim: Wiley-VCH.
2 Katz, E. ed. (2012). *Biomolecular Information Processing – From Logic Systems to Smart Sensors and Actuators*. Weinheim: Wiley-VCH.
3 Katz, E. ed. (2014). *Implantable Bioelectronics: Devices, Materials, and Applications*. Weinheim: Wiley-VCH.

January, 2018

Evgeny Katz
Potsdam, NY, USA

1

Introduction

Modified electrodes functionalized with various organic monolayers and thin films attached to conducting surfaces have found numerous applications in electrocatalysis, sensors, and fuel cells [1–7]. Particularly, active research has been directed to the applications of modified electrodes in different bioelectrochemical systems [8, 9], including biosensors [10–13] and biofuel cells [14–17]. In the past two decades, different modified electrodes functionalized with signal-responsive molecules [18], polymers [19], or supra-molecular complexes [20] were developed to facilitate the "switch-on-demand" electrochemical properties of the electrode surfaces. Their applications in switchable biosensors [21], fuel cells [22], and electrochemical systems processing information [23] have been suggested. Various physical or/and chemical signals as well as their combinations were used to switch electrochemical properties of the modified interfaces between active and inactive states for specific electrochemical, electrocatalytic, and bioelectrocatalytic reactions. Light signals (irradiation of electrodes with visible or ultraviolet light) [24–31], magnetic field applied at electrode surfaces loaded with magnetic nanoparticles or magnetic nanowires [32–43], and electrical potentials producing chemical changes at the electrode surfaces [44–48] were used to reversibly alternate electrochemical properties of the modified electrodes. Chemical [29, 49–51] or biochemical [52] signals resulting in reversible changes of the interfacial properties were also used to switch the electrode activity ON/OFF for specific electrochemical transformations. Particularly, important progress has been achieved in switchable bioelectronics, where signal-controlled electrodes have been used for adaptable features of novel bioelectronic devices [53]. This book gives an overview of the different signal-responsive electrochemical interfaces and complex multicomponent electrochemical systems, particularly emphasizing the importance of scaling-up the complexity of the signal-processing systems.

References

1 Albery, W.J. and Hillman, A.J. (1981). *Annu. Rep. Prog. Chem. Sect. C: Phys. Chem.* 78: 377–437.

2 Murray, R.W. (1984). Chemically modified electrodes. In: *Electroanalytical Chemistry*, vol. 13 (ed. A.J. Bard), 191–368. New York: Marcel Dekker.

Signal-switchable Electrochemical Systems: Materials, Methods, and Applications, First Edition. Evgeny Katz.

3 Murray, R.W. (1980). *Acc. Chem. Res.* 13: 135–141.
4 Wrighton, M.S. (1986). *Science* 231: 32–37.
5 Abruña, H.D. (1988). *Coord. Chem. Rev.* 86: 135–189.
6 Chen, D. and Li, J.H. (2006). *Surf. Sci. Rep.* 61: 445–463.
7 Zen, J.M., Kumar, A.S., and Tsai, D.-M. (2003). *Electroanalysis* 15: 1073–1087.
8 Rusling, J.F. and Forster, R.J. (2003). *J. Colloid Interface Sci.* 262: 1–15.
9 Willner, I. and Katz, E. (2000). *Angew. Chem. Int. Ed.* 39: 1180–1218.
10 Wang, J. (1999). *J. Pharm. Biomed. Anal.* 19: 47–53.
11 Wang, J. (2008). *Talanta* 75: 636–641.
12 Gooding, J.J. (2008). *Electroanalysis* 20: 573–582.
13 Wollenberger, U., Spricigo, R., Leimkuhler, S., and Schronder, K. (2008). Protein electrodes with direct electrochemical communication. In: *Biosensing for the 21st Century*, Advances in Biochemical Engineering/Biotechnology, vol. 109 (ed. R. Renneberg and F. Lisdat), 19–64. New York: Springer.
14 Moehlenbrock, M.J. and Minteer, S.D. (2008). *Chem. Soc. Rev.* 37: 1188–1196.
15 Davis, F. and Higson, S.P.J. (2007). *Biosens. Bioelectron.* 22: 1224–1235.
16 Bullen, R.A., Arnot, T.C., Lakeman, J.B., and Walsh, F.C. (2006). *Biosens. Bioelectron.* 21: 2015–2045.
17 Barton, S.C., Gallaway, J., and Atanassov, P. (2004). *Chem. Rev.* 104: 4867–4886.
18 Katz, E., Willner, B., and Willner, I. (1997). *Biosens. Bioelectron.* 12: 703–719.
19 Motornov, M., Sheparovych, R., Katz, E., and Minko, S. (2008). *ACS Nano* 2: 41–52.
20 Flood, A.H., Ramirez, R.J.A., Deng, W.Q. et al. (2004). *Aust. J. Chem.* 57: 301–322.
21 Laocharoensuk, R., Bulbarello, A., Hocevar, S.B. et al. (2007). *J. Am. Chem. Soc.* 129: 7774–7775.
22 Wang, J., Musameh, M., Laocharoensuk, R. et al. (2006). *Electrochem. Commun.* 8: 1106–1110.
23 Shipway, A.N., Katz, E., and Willner, I. (2001). Molecular memory and processing devices in solution and on surfaces. In: *Structure and Bonding*, Molecular Machines and Motors, vol. 99 (ed. J.-P. Sauvage), 237–281. Berlin: Springer-Verlag.
24 Lion-Dagan, M., Katz, E., and Willner, I. (1994). *J. Am. Chem. Soc.* 116: 7913–7914.
25 Katz, E., Lion-Dagan, M., and Willner, I. (1995). *J. Electroanal. Chem.* 382: 25–31.
26 Willner, I., Lion-Dagan, M., Marx-Tibbon, S., and Katz, E. (1995). *J. Am. Chem. Soc.* 117: 6581–6592.
27 Willner, I., Lion-Dagan, M., and Katz, E. (1996). *Chem. Commun.* 623–624.
28 Doron, A., Portnoy, M., Lion-Dagan, M. et al. (1996). *J. Am. Chem. Soc.* 118: 8937–8944.
29 Doron, A., Katz, E., Tao, G.L., and Willner, I. (1997). *Langmuir* 13: 1783–1790.
30 Liu, N.G., Dunphy, D.R., Atanassov, P. et al. (2004). *Nano Lett.* 4: 551–554.
31 Liu, Z.F., Hashimoto, K., and Fujishima, A. (1990). *Nature* 347: 658–660.
32 Hsing, I.M., Xu, Y., and Zhao, W.T. (2007). *Electroanalysis* 19: 755–768.
33 Katz, E., Baron, R., and Willner, I. (2005). *J. Am. Chem. Soc.* 127: 4060–4070.
34 Katz, E., Sheeney-Haj-Ichia, L., Basnar, B. et al. (2004). *Langmuir* 20: 9714–9719.

35 Willner, I. and Katz, E. (2003). *Angew. Chem. Int. Ed.* 42: 4576–4588.
36 Katz, E., Sheeney-Haj-Ichia, L., and Willner, I. (2002). *Chem. Eur. J.* 8: 4138–4148.
37 Hirsch, R., Katz, E., and Willner, I. (2000). *J. Am. Chem. Soc.* 122: 12053–12054.
38 Wang, J. and Kawde, A.N. (2002). *Electrochem. Commun.* 4: 349–352.
39 Laocharoensuk, R., Bulbarello, A., Mannino, S., and Wang, J. (2007). *Chem. Commun.* 3362–3364.
40 Wang, J. (2008). *Electroanalysis* 20: 611–615.
41 Loaiza, O.A., Laocharoensuk, R., Burdick, J. et al. (2007). *Angew. Chem. Int. Ed.* 46: 1508–1511.
42 Wang, J., Scampicchio, M., Laocharoensuk, R. et al. (2006). *J. Am. Chem. Soc.* 128: 4562–4563.
43 Lee, J., Lee, D., Oh, E. et al. (2005). *Angew. Chem. Int. Ed.* 44: 7427–7432.
44 Zheng, L. and Xiong, L. (2006). *Colloids Surf., A* 289: 179–184.
45 Riskin, M., Basnar, B., Katz, E., and Willner, I. (2006). *Chem. Eur. J.* 12: 8549–8557.
46 Riskin, M., Basnar, B., Chegel, V.I. et al. (2006). *J. Am. Chem. Soc.* 128: 1253–1260.
47 Chegel, V.I., Raitman, O.A., Lioubashevski, O. et al. (2002). *Adv. Mater.* 14: 1549–1553.
48 Le, X.T., Jégou, P., Viel, P., and Palacin, S. (2008). *Electrochem. Commun.* 10: 699–703.
49 Hou, K.Y., Yu, L., Severson, M.W., and Zeng, X.Q. (2005). *J. Phys. Chem. B* 109: 9527–9531.
50 Tokarev, I., Orlov, M., Katz, E., and Minko, S. (2007). *J. Phys. Chem. B* 111: 12141–12145.
51 Tam, T.K., Ornatska, M., Pita, M. et al. (2008). *J. Phys. Chem. C* 112: 8438–8445.
52 Tam, T.K., Zhou, J., Pita, M. et al. (2008). *J. Am. Chem. Soc.* 130: 10888–10889.
53 Parlak, O. and Turner, A.P.F. (2016). *Biosens. Bioelectron.* 76: 251–265.

2

Magneto-switchable Electrodes and Electrochemical Systems

2.1 Introduction

This chapter overviews various electrochemical systems with switchable features that can be controlled by external magnetic fields applied to magnetic micro/nanospecies. The use of magnetic micro/nanospecies (e.g., nanoparticles, nanowires, nanosheets) [1–6] has been particularly important for the development of novel magneto-switchable electrodes with unique and unusual properties [7–13]. Applying a magnetic field to magnetic species with redox, electrocatalytic, or bioelectrocatalytic properties and moving them around allowed their different arrangements on electrode surfaces, thus changing their electrochemical responses, switching them ON and OFF resulting in many interesting features, Figure 2.1. While the exact description of the exemplified systems can be found in original research papers, this richly illustrated chapter aims at providing conceptual explanations to summarize the up to date developments in this field. The Appendix organized at the end of the chapter addresses those readers specifically interested in synthetic procedures used for preparation and characterization of nanosized magnetic materials.

2.2 Lateral Translocation of Magnetic Micro/nanospecies on Electrodes and Electrode Arrays

One of the earliest examples of the magneto-switchable bioelectrochemical systems was based on lateral translocation of deoxyribonucleic acid (DNA)-functionalized magnetic microspheres (super-paramagnetic polystyrene beads, ca. 1 μm, with included Fe_3O_4 nanoparticles) along an electrode array composed of two conducting areas ("left" and "right" electrodes), both with the applied potential of oxidizing DNA molecules [14], Figure 2.2. The magnetic microspheres chemically modified with DNA oligomers (GGC CGA CTC ACT GCG CGT CTT CTG TCC CGC CTT TTT CG (**1**); note that the used oligomer is rich with guanine bases) demonstrated chronopotentiometric responses corresponding to the irreversible oxidation of guanine nucleobases in the DNA molecules. When the DNA-magnetic species were collected at the "left" electrode by positioning an external magnet below that electrode, they demonstrated the

Signal-switchable Electrochemical Systems: Materials, Methods, and Applications, First Edition. Evgeny Katz.

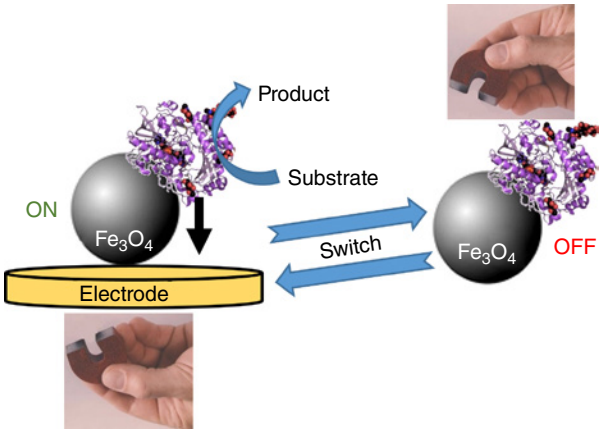

Figure 2.1 Magneto-controlled switchable bioelectrocatalytic process – a general concept.

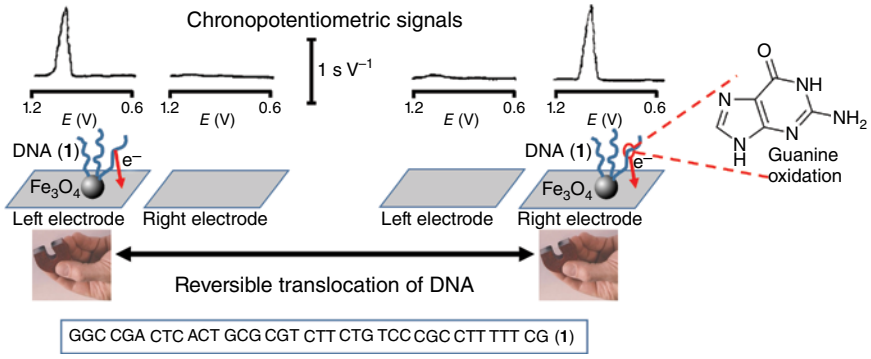

Figure 2.2 Reversible switching of the DNA oxidation upon magneto-induced lateral translocation of the DNA-functionalized Fe_3O_4 magnetic particles. Chronopotentiometric responses of the "left" and "right" electrodes are shown in the presence and absence of the particles. Amount of magnetic particles, 100 µg; DNA-oligomer (**1**) structure is shown (note that the used oligonucleotide is rich with oxidizable guanine bases); pre-treatment potential, +1.7 V for 10 s; stripping current, +5 µA (between 0.6 and 1.2 V vs Ag/AgCl reference electrode). *Source:* Wang and Kawde 2002 [14]. A fragment of this figure is adapted with permission from Elsevier.

electrochemical response on the "left" electrode leaving the "right" electrode mute and not responsive to the applied oxidative potential. Repositioning the external magnet to the "right" electrode resulted in the switch of the electrochemical response to that electrode due to translocation of the DNA-functionalized magnetic species following the magnet. The process of switching the positioning of the DNA molecules and their electrochemical responses between the "left" and "right" electrodes was repeatedly cycled and reversible, thus demonstrating effective translocation of the DNA-functionalized magnetic species following the changes in the magnet position. The switchable magneto-controlled DNA-based electrochemical system was suggested by the authors [14] as a platform "for stimulating charge transfer through DNA, and for other genoelectronic applications."

While the concept illustrated by this system is indeed very interesting, the drawback of the system is the electrochemically irreversible and chemically destructive oxidation of guanine bases in the DNA oligomer.

Another magneto-switchable system based on the lateral translocation of redox-functionalized magnetic species included Fe_3O_4 microparticles (ca. 1 μm average diameter) modified with quinone molecules [15]. The advantage of this system, particularly when compared with the DNA oxidation described above, is the reversible electrochemical process of the used quinone redox species. Two different quinone molecules were used to study the magneto-switchable properties of the system. In the first example [15], biologically important pyrroloquinoline quinone (PQQ) covalently bound to the magnetic particles through an amino-silane shell was reversibly translocated between the "left" and "right" electrodes by moving an external magnet similarly to the system described above. The electrochemically reversible cyclic voltammogram responses were obtained at the "left" and "right" electrodes depending on the magnet position. Since the PQQ molecules are well known catalytic species for β-nicotinamide adenine dinucleotide (NADH) oxidation [16], the primary electrochemical response of PQQ was extended to the electrocatalytic NADH oxidation observed on the "left" and "right" electrodes by moving the external magnet to the corresponding positions below these electrodes [15]. The present example is particularly important because it demonstrated the cascading electrocatalytic reaction that was controlled by the positioning of the external magnet. In the second example [15], amino-naphthoquinone (**2**) was covalently attached to the magnetic microparticles, Figure 2.3A. Electrochemical reduction of the immobilized naphthoquinone in the presence of oxygen resulted in the electrocatalytic O_2 reduction and formation of H_2O_2, which was coupled with the biocatalytic oxidation of 3,3′,5,5′-tetramethylbenzidine (**3**) to give the insoluble product (**4**), Figure 2.3B. This process was biocatalyzed by horseradish peroxidase enzyme (HRP, E.C. 1.11.1.7), which resulted in deposition of the insoluble product (**4**) on the electrode surface. Importantly, the electro-biocatalytically produced precipitate was deposited at the location of the magnetic particles controlled by the magnet positioning, thus resulting in the magneto-controlled patterning of the electrode surface, Figure 2.3C.

A similar process, but using luminol (**5**) as an oxidizable substrate for HRP, resulted in biocatalytically induced luminescence controlled by the magnet position [17]. In this study, the amino-naphthoquinone (**2**)-modified magnetic microparticles (ca. 1 μm average diameter) were reversibly moved between conducting and nonconducting domains by moving the external magnet, Figure 2.4A. When the particles were concentrated on the conducting Au electrode, the naphthoquinone molecules were electrochemically reduced, subsequently producing H_2O_2 in the electrocatalytic oxygen reduction process. The generated H_2O_2 activated HRP-biocatalyzed oxidation of luminol to the light-emitting excited state of 3-aminophthalate (**6**), resulting in the luminescence process. When the magnetic particles were relocated to the nonconducting glass domain, the electrocatalytic process was stopped and the luminescence was not observed. The electrocatalytic oxygen reduction in the presence of the quinone-functionalized magnetic particles on the Au electrode surface was observed by

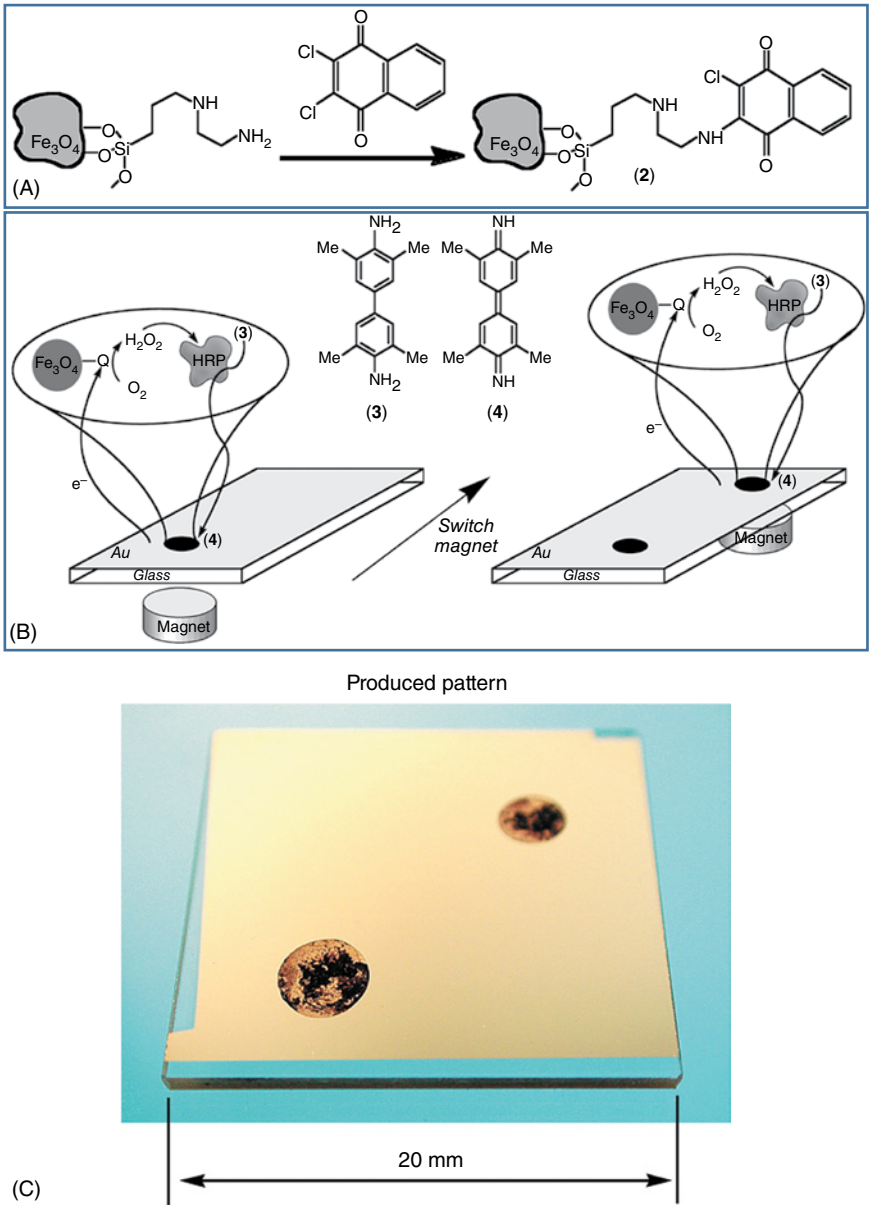

Figure 2.3 (A) Modification of magnetic Fe_3O_4 microparticles (ca. 1 μm diameter) with naphthoquinone (**2**). (B) Magneto-controlled patterning of a Au electrode surface upon formation of an insoluble product (**4**) of a biocatalytic reaction triggered by the electrocatalytic formation of H_2O_2 in the presence of naphthoquinone (**2**)-functionalized magnetic particles. (C) Pattern produced on the Au electrode by the electrocatalytic process using the naphthoquinone (**2**)-functionalized magnetic particles, 10 mg, HRP, 1 mg mL^{-1}, and substrate (**3**), 3×10^{-4} M. Background electrolyte: 0.1 M tris-buffer, pH 7.5, was saturated with air. The potential, −0.5 V (vs SCE), was applied for 3 min on the electrode to produce the first spot, then the potential was switched off, the magnetic particles were moved by the external magnet, and the potential −0.5 V was reapplied for 3 min to produce the second spot. *Source:* Katz and Willner 2002 [15]. The figure is adapted with permission from Elsevier.

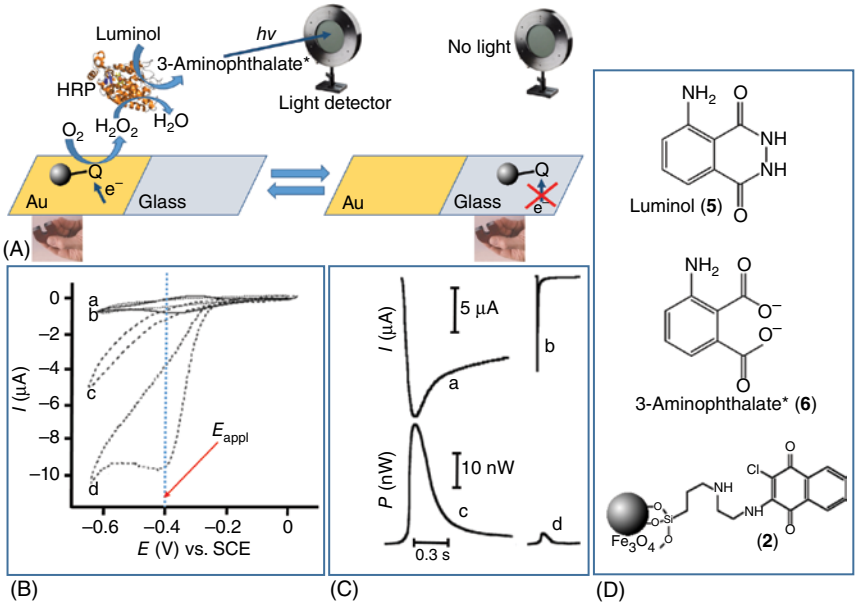

Figure 2.4 (A) Magneto-controlled electrobiochemiluminescence. Note that the light emission was observed only when the quinone-functionalized magnetic particles were located on the electrode surface. (B) Cyclic voltammograms of: (a) the cystamine-modified Au electrode under Ar (dashed line); (b) the naphthoquinone (**2**)-modified particles (10 mg) magnetically attracted to the electrode surface under Ar (solid line); (c) the cystamine-modified Au electrode under air in the absence of magnetic particles; and (d) the naphthoquinone (**2**)-modified particles (10 mg) magnetically attracted to the electrode surface under air. The vertical dash line shows the potential of −0.4 V (vs SCE), which was applied to induce the electrobioluminescence – compare electrocatalytic (curve d) and non-catalytic (curve c) currents at this potential. All experiments were recorded in 0.1 M phosphate buffer, pH 7.0, potential scan rate, 10 mV s^{-1}. (C) Magneto-switchable electrocatalytic generation of biochemiluminescence in a system consisting of the naphthoquinone (**2**)-functionalized magnetic particles (10 mg), luminol (1 μM), and HRP (1 mg mL^{-1}). Top curves: chronoamperometric transients upon application of potential steps from 0.0 to −0.4 V (vs SCE) on the cystamine-modified Au electrode: (a) current transient measured when the naphthoquinone (**2**)-functionalized particles are positioned on the Au electrode by the external magnet; (b) current transient measured when the particles are translocated to the nonconductive glass support by the external magnet. Note that the short current pulse observed in the absence of the quinone-modified particles corresponds mostly to the capacitance current. Bottom curves: light (measured by the light detector as power) emitted from the system upon the application of the respective chronoamperometric transients: (c, d) in the presence and absence of the particles on the Au electrode, respectively. Note that the light emission intensity correlates with the produced current. All measurements were performed in 0.1 M phosphate buffer, pH 7.0, system equilibrated with air. (D) Structures of luminol, 3-aminophthalate (excited state) and naphthoquinone (**2**)-functionalized magnetic particles. *Source:* Sheeney-Haj Ichia et al. 2002 [17]. A fragment of this figure is adapted with permission from Royal Society of Chemistry.

cyclic voltammetry, Figure 2.4B, curve d. The non-catalyzed oxygen reduction with a smaller cathodic current was obtained when the magnetic particles were relocated to the nonconducting glass domain, Figure 2.4B, curve c. The light emission resulting from the bioelectrocatalytic process followed the current

transients observed by chronoamperometry, Figure 2.4C. Figure 2.4D shows the structures of the reacting species. Note that the potential applied on the Au electrode (left conducting domain), −0.4 V (vs saturated calomel electrode (SCE)), was sufficient for the electrocatalytic process in the presence of the quinone-modified magnetic particles, but not enough for non-catalytic oxygen reduction in their absence, thus inhibiting the light emission in the absence of magnetic particles on the electrode surface. The present example illustrated another complex electro-biocatalytic process effectively switched ON and OFF by the external magnetic field.

Lateral translocation of magnetic species coupled with electrocatalytic processes and controlled by positioning of the external magnet was recently extended to the use of novel magnetic nanospecies – iron-rich graphene sheets [18]. After discovering graphene, a one-layer thick, two-dimensional material with an sp^2-bonded carbon network arranged in a honeycomb lattice [19], various derivative materials have been synthesized, including metal-doped graphene hybrid materials with different properties depending on the used metal dopants [20]. An iron-doped thermally reduced graphene oxide (Fe-TRGO) was prepared and was used to trigger and enhance electrochemical reactions on electrodes with the switchable positioning of Fe-TRGO controlled by the external magnetic field [18], Figure 2.5. Using its magnetic properties, the composite Fe-TRGO nanomaterial was reversibly translocated by moving an external magnet between two positions: one located below a screen-printed electrode (SPE) and the other away from the conducting surface, Figure 2.5A. When Fe-TRGO was positioned on the conducting surface of SPE, it electrocatalyzed the oxidation of ascorbic acid, AA (**7**), to yield dehydroascorbic acid, DAA (**8**), thus demonstrating decreasing overpotential in the formation of the anodic current in the cyclic voltammogram, Figure 2.5B, as compared with the noncatalyzed process in the absence of Fe-TRGO on the electrode surface, Figure 2.5C. The anodic current corresponding to the AA oxidation was also increased due to the increase of the conducting surface in the presence of Fe-TRGO nanomaterial on the SPE surface. The changes of the peak current, Figure 2.5D, and peak potential, Figure 2.5E, in the cyclic voltammograms were reversible upon moving Fe-TRGO to and from the electrode surface by applying an external magnetic field. This system is particularly interesting and potentially useful for future applications since Fe-TRGO combines two properties in one composite material: magneto-sensitivity to allow its translocation by an external magnetic field and electrocatalytic properties to enhance electrochemical processes when Fe-TRGO locates on the electrode surface.

In the examples discussed, magnetic nanospecies were modified with some additional components to have electrocatalytic properties (e.g., quinone molecules chemically attached to magnetic particles or Fe-dopant included in Fe-TRGO hybrid material). However, Ni particles demonstrating magnetic and electrocatalytic features can be used for magneto-switchable electrocatalysis without any additional modification, thus eliminating the need for their functionalization with catalytic entities [21]. The magneto-induced lateral translocation of Ni particles (Ni metal powder 325 mesh) between "left" and "right" electrodes allowed electrocatalytic oxidation of alcohols, sugars, and amino acids on-demand at any of the used electrodes. This represented the first example of

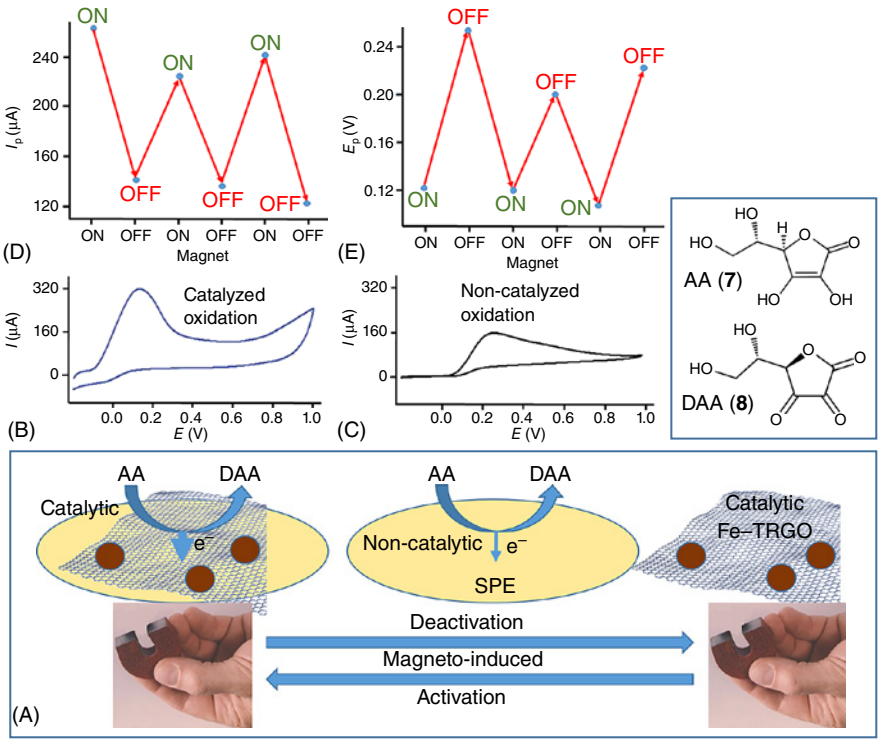

Figure 2.5 (A) Reversible activation and deactivation of electrocatalytic processes on a screen-printed electrode (SPE) upon magneto-induced lateral translocation of iron-doped thermally reduced graphene oxide (Fe-TRGO). Ascorbic acid (AA, **7**) is electrocatalytically oxidized to dehydroascorbic acid (DAA, **8**) when Fe-TRGO is located on the SPE surface (left) and non-catalytically oxidized when Fe-TRGO is removed from the electrode surface (right). (B) Cyclic voltammogram corresponding to the AA electrocatalytic oxidation in the presence of Fe-TRGO. (C) Cyclic voltammogram corresponding to the AA non-catalytic oxidation in the absence of Fe-TRGO (note smaller current and more positive anodic peak comparing with the cyclic voltammogram show in B). Potential scan rate, 100 mV s^{-1}. The potentials are shown vs Ag/AgCl reference electrode. (D) Reversible variation of the peak current upon activation (ON) and deactivation (OFF) of the electrocatalytic process. (C) Reversible variation of the peak potential upon activation (ON) and deactivation (OFF) of the electrocatalytic process. *Source:* Lim et al. 2014 [18]. A fragment of this figure is adapted with permission from Royal Society of Chemistry.

the concept of magneto-switchable electrochemistry where the magnetic and catalytic properties are combined in the same material.

2.3 Vertical Translocation of Magnetic Micro/Nanospecies to and from Electrode Surfaces

Magnetic particles (Fe_3O_4, saturated magnetization ca. 65 emu g^{-1}, ca. 1 μm average diameter) functionalized with chemically attached redox species were reversibly moved by an external magnetic field from the solution to the electrode

interface and back to the solution by placing an external magnet (NdFeB/Zn-coated magnet with a remanent magnetization of 10.8 kG) below and above the electrode, respectively, Figure 2.6A. While being suspended in the solution, the redox-functionalized magnetic particles were unable to interact directly with the electrode surface, thus demonstrating no electrochemical response. Upon magneto-induced translocation to the electrode surface they were associated with the conducting support and demonstrated their redox activity. Electron transfer properties of redox-functionalized magnetic particles deposited on the electrode surface were characterized by cyclic voltammetry. For example, Fe_3O_4 magnetic particles were silanized with [3-(2-aminoethyl)aminopropyl]trimethoxysilane to yield amino groups that were used for covalent immobilization of PQQ (**9**), via carbodiimide coupling procedure [9]. Magneto-induced translocation of the PQQ-modified particles to the electrode surface allowed their direct contacting with the electrode resulting in the reversible electrochemical process with the potential $E^\circ = -0.16$ V (vs SCE, pH 8.0), Figure 2.6B, curve a. Variation of the potential scan rate upon cyclic voltammetry measurements resulted in the linear increase of the peak current, I_p, Figure 2.6C, inset, thus demonstrating features typical for the surface-confined redox species [22]. The peak-to-peak separation, ΔE_p, in the cyclic voltammograms measured with different potential scan rates, ν, Figure 2.6C, followed the function expected from Laviron's theory [23, 24] and resulted in the electron transfer rate constant, k_{et}, of ca. $2\,s^{-1}$ [9]. When the PQQ-modified magnetic particles were lifted up to the solution, Figure 2.6A, the cyclic voltammogram showed only small response from a minor fraction of the particles stuck on the surface, Figure 2.6B, curve b, thus demonstrating that the majority of the particles can be disconnected from the electrode surface by repositioning the external magnet above the electrode surface. Overall, the redox potential of the PQQ molecules bound to the magnetic particles and the electron transfer kinetics for the species resting on the electrode surface were similar to those found for the monolayer-immobilized PQQ [25], thus demonstrating no problems for the interfacial electron transfer and charge propagation through the redox-pool around the particles.

The experiments were extended to other redox molecules covalently bound to Fe_3O_4 particles for demonstrating the reversible activation and inhibition of their electrochemical reactions upon switching the external magnetic field by repositioning of the magnet below and above the electrode surface, respectively, [13, 26] Figure 2.7. Two examples of redox molecules with different redox potentials and different numbers of electrons involved in the oxidation/reduction processes have been selected. Amino-naphthoquinone (**2**) ($E^\circ = -0.39$ V vs SCE at pH = 7.0 demonstrating $2e^-/2H^+$ redox process typical for quinones in aqueous solutions [27]), Figure 2.7A, and a ferrocene derivative (**10**) ($E^\circ = 0.32$ V vs SCE, demonstrating pH-independent $1e^-$ redox process typical for ferrocene derivatives [28]), Figure 2.7B, have been covalently attached to the magnetic particles and moved up and down in the electrochemical cell by repositioning an external magnet. The electrochemical responses of the redox-functionalized magnetic particles (measured as differential pulse voltammograms, DPVs), Figure 2.7C,D, were very small when the particles were suspended in the solution being away from the electrode surface. The observed small peaks in the

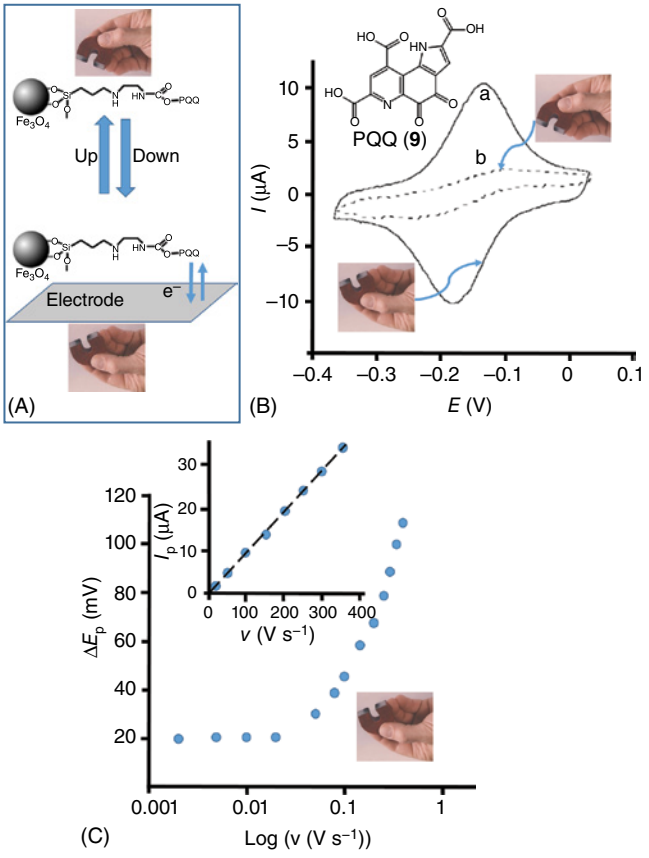

Figure 2.6 (A) Reversible activation/inhibition of the electrochemical reaction of PQQ (**9**) covalently bound to Fe_3O_4 microparticles (ca. 1 μm diameter) upon their vertical translocation up and down with help of an external magnet. Note that the PQQ-modified magnetic particles are disconnected from the electrode surface in the up-position of the magnet, while their translocation down results in their deposition on the electrode surface. (B) Cyclic voltammograms corresponding to the electrode surface with the magnetically attracted PQQ-modified particles (a) and to the electrode surface after their magneto-induced removal (b); the small wave observed in the latter cyclic voltammogram (b) is due to the incomplete removal of the particles. The data were obtained in Tris buffer (0.1 M, pH 8.0) in the presence of $CaCl_2$ (10 mM) under argon. Potential scan rate, 100 mV s^{-1}. The potentials are shown vs SCE. (C) Dependence of the peak-to-peak separation, ΔE_p, on the potential scan rate, *v*, observed in the cyclic voltammograms of PQQ-functionalized magnetic particles attracted to the Au electrode. Inset: dependence of the peak current, I_p, on the potential scan rate. *Source:* Katz et al. 2002 [9]. A fragment of this figure is adapted with permission from John Wiley and Sons.

DPVs, Figure 2.7C,D, curves b, originated from the incomplete removal of the particles from the electrode surface. On the other hand, the attraction of the particles to the electrode surface resulted in their direct electrical contact with the electrode, thus facilitating the electron transfer processes and resulting in much higher peaks in the DPVs, Figure 2.7C,D, curves a. The reversible translocation of the particles between the surface-confined and solution-suspended positions resulted in reversible changes of the peak currents, I_p, Figure 2.7C,D,

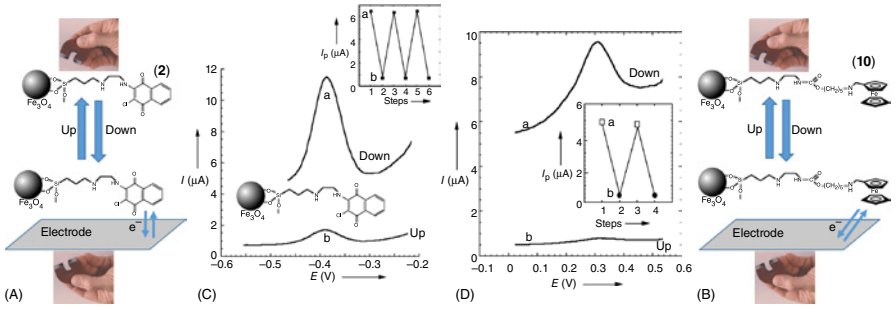

Figure 2.7 Reversible activation/inhibition of electrochemical reactions of the redox species covalently bound to Fe_3O_4 microparticles (ca. 1 μm diameter) upon their vertical translocation with help of an external magnet: translocation to and from the electrode surface is shown for naphthoquinone (**2**)-modified particles (A) and ferrocene (**10**)-modified particles (B) in the left and right schemes, respectively. (C) Differential pulse voltammograms (DPVs) recorded for the naphthoquinone (**2**)-modified particles magnetically attracted to the electrode surface (curve a) and removed from it (curve b). (D) DPVs recorded for the ferrocene (**10**)-modified particles magnetically attracted to the electrode surface (curve a) and removed from it (curve b). Potential scan rate, 20 mV s^{-1}. The potentials are shown vs SCE. Insets show reversible variation of the peak current upon stepwise attraction of the particles to (a) and removal from (b) the electrode surface. *Source:* Katz et al. 2002 [9]. A fragment of this figure is adapted with permission from John Wiley and Sons.

insets. The obtained results successfully demonstrated that the reversible switching of the electrochemical reactions can be realized with very different redox species bound to Fe_3O_4 particles.

In addition to the magneto-induced reversible activation–inactivation of the redox reactions for the species chemically attached to the particles, magnetic particles were proven to be valuable for triggering electrocatalytic and bioelectrocatalytic cascades mediated by the redox species [13], Figure 2.8. In order to exemplify the electrocatalytic reactions switchable by the external magnetic field, the magnetic particles have been covalently functionalized with PQQ [13], which is a well-known electrocatalyst for NADH oxidation [16] and then the PQQ-modified magnetic particles were moved up and down with the external magnetic field to switch OFF and ON the electrocatalytic NADH oxidation, respectively, Figure 2.8A. (Note similar experiments with the PQQ-modified magnetic particles laterally translocated with an external magnet between "left" and "right" electrodes [15].) The cyclic voltammograms observed for different positioning of the particles demonstrated the mute electrochemical response and effective electrocatalytic wave when the particles were solution-suspended and surface-confined, respectively, Figure 2.8C. The reversible activation of the NADH electrocatalytic oxidation was achieved upon stepwise application of the external magnetic field below and above the electrode, Figure 2.8C, inset. Another example included the bioelectrocatalytic oxidation of glucose in the presence of glucose oxidase (GOx; E.C. 1.1.3.4) mediated by a ferrocene derivative (**10**) bound to the magnetic particles [13, 26], Figure 2.8B. Since GOx cannot communicate directly with an electrode surface [29], a mediating process in the presence of the ferrocene derivative is needed to activate the bioelectrocatalytic reaction [30]. In the present example, the bioelectrocatalytic reaction was followed by cyclic voltammetry and it was activated only when the ferrocene-modified magnetic particles were associated with the electrode surface, being attracted by the magnet located below the electrode, Figure 2.8D, curve a. When the particles were suspended in the solution, the ferrocene mediator was not able to transport electrons from GOx to the electrode surface, thus demonstrating the inhibited process, Figure 2.8D, curve b. The reversible activation/inhibition of the bioelectrocatalytic process was observed upon stepwise translocation of the particles between the surface-confined and solution-suspended position by applying the external magnetic field below and above the electrode, respectively, Figure 2.8D, inset. While the present example demonstrated the oxidative bioelectrocatalytic pathway controlled by the external magnetic field, another system was designed to exemplify the reductive bioelectrocatalysis switchable by a magnetic field [9, 13, 26]. In that system a viologen derivative (*N*-methyl-*N*′-(dodecanoic acid)-4,4'-bipyridinium, $E^\circ = -0.56$ V vs SCE [31]) was bound covalently to the Fe_3O_4 magnetic particles and was used to mediate reduction of NO_3^- biocatalyzed by nitrate reductase (E.C. 1.6.6.2), thus performing the reductive bioelectrocatalytic pathway. Similarly to the previous system, the process was switched by repositioning the external magnet to bring the particles to the electrode surface and resuspend them in the solution, thus switching ON and OFF of the process, respectively [9, 26].

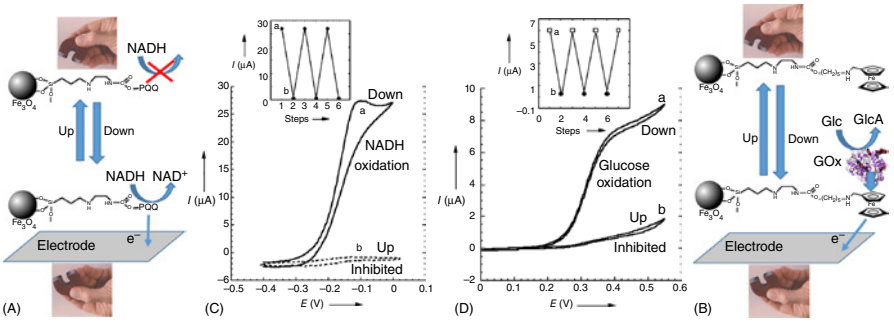

Figure 2.8 Reversible activation/inhibition of electrocatalytic reactions mediated by the redox species covalently bound to Fe_3O_4 microparticles (ca. 1 μm diameter) upon their vertical translocation with help of an external magnet: translocation to and from the electrode surface is shown for PQQ-modified particles in the presence of NADH (A) and ferrocene-modified particles in the presence of GOx and glucose (B) in the left and right schemes, respectively. (C) Cyclic voltammograms recorded for the PQQ-modified particles in the presence of NADH (50 mM) magnetically attracted to the electrode surface (curve a) and removed from it (curve b). Potential scan rate, 10 mV s^{-1}. (D) Cyclic voltammograms recorded for the ferrocene-modified particles in the presence of GOx (1 mg mL^{-1}) and glucose (10 mM) magnetically attracted to the electrode surface (curve a) and removed from it (curve b). Potential scan rate, 5 mV s^{-1}. The potentials are shown vs SCE. Insets show reversible variation of the electrocatalytic current upon stepwise attraction of the particles to (a) and removal from (b) the electrode surface. *Source:* Katz et al. 2002 [9]. A fragment of this figure is adapted with permission from John Wiley and Sons.